2023 IEEE 26th International Conference on
Intelligent Transportation Systems (ITSC)
24-28 September 2023. Bilbao, Bizkaia, Spain

Identifying Vehicle Interaction at Urban Intersections: A Comparison of Proximity Resistance, Time-to-Collision, and Post-Encroachment-Time

Yiru Jiao[1*], Simeon C. Calvert[1], Sander van Cranenburgh[2], and Hans van Lint[1]

2023 IEEE 26th International Conference on Intelligent Transportation Systems (ITSC) | 979-8-3503-9946-2/23/$31.00 ©2023 IEEE | DOI: 10.1109/ITSC57777.2023.10422682

***Abstract*— Interactions between vehicles are extensive at intersections and significantly influence traffic efficiency and safety. Identifying where vehicle interaction occurs at intersections can provide insights for improving designs of and operations on intersections. Conflict indicators like Time-to-Collision (TTC) and Post-Encroachment-Time (PET) have been used to identify vehicle interaction. However, their sole focus on conflicts and potential collisions overlooks cooperative interaction such as waiting for others to pass first. This paper proposes using Proximity Resistance (PR) to identify vehicle interaction at urban intersections. PR measures two-dimensional spacing between vehicles, thus can identify interacting vehicles when their spacing is smaller than typically considered desirable by the drivers. With empirical analysis at an unsignalised urban intersection, this paper demonstrates the effectiveness of PR in identifying cooperative vehicle interaction beyond conflicts. Thereby, this study contributes to a more comprehensive understanding of vehicle interaction at urban intersections.**

***Index Terms*— Vehicle interaction, urban intersection, trajectory analysis, proximity resistance**

I. Introduction

Urban intersections play a key role in accommodating traffic from different directions. Unlike straight corridors, when passing through intersections, vehicles interact with one another not only longitudinally by such as car following, but also laterally during merging and turning [1]. Assessing the practical use of an intersection is vital for effective traffic management [2]. Although current theoretical design and simulation tests are valuable in the development phase prior to an intersection's actual use, they are insufficient for capturing the complex two-dimensional interactions between vehicles in real-world traffic. Empirical analysis is thus necessary to improve the traffic safety and efficiency at urban intersections, by identifying where vehicle interactions happen the most in real use. This is being promoted by the collection of trajectory data. With rapid advances in computer vision for object detection and tracking, automatically extracting accurate vehicle trajectories is increasingly feasible [3,4], and the extraction errors has been reduced to less than 0.2 m for aerial videos [5,6].

In road safety domain, vehicle interactions refer to situations where two or more road users approach each other and are within sufficient proximity in space and time [7,8]. With increasing degree of spatial and temporal proximity, vehicle interaction includes a continuum of safety related events: undisturbed passages, potential conflicts, slight conflicts, serious conflicts, and accidents [9]. As such, Time-to-Collision (TTC) and Post-Encroachment-Time (PET) are widely employed indicators of interaction. TTC estimates the time remaining before a collision if two vehicles continue on their current paths and speeds, whereas PET measures the time interval between one vehicle leaving a conflict zone and another vehicle entering the same zone.

However, vehicle interactions do not necessarily lead to conflicts, but can also resolve potential conflicts and actively avoid potential hazards [10]. Using conflict indicators to identify vehicle interactions is thus limited. First, TTC is effective in detecting rear-end conflicts between vehicles following one another on straight corridors [11–13], but its validity at intersections is unsure [14]. Second, although TTC can be adapted to two-dimensional scenarios and PET is designed for traffic conflicts at intersections [15–17], they both are exclusively focused on potential conflicts and collisions. Such focus may overlook cooperative interactions that are beneficial to traffic efficiency and safety, e.g., one vehicle actively moving away from another vehicle to create space for it.

In this study, we propose using Proximity Resistance (PR) as an alternative to conflict-focused indicators like TTC and PET for identifying vehicle interaction. PR was proposed in our previous study [18]. Based on the accumulated presence of vehicles in different traffic conditions, PR quantifies the degree to which the current spacing between two vehicles is larger or smaller than that is typically considered desirable. If the spacing (i.e., proximity) in a certain condition is smaller than desired, it indicates a higher likelihood that the vehicles are engaged in interaction. We argue that PR is more representative for general vehicle interaction at intersections for the following reasons.

- PR evaluates two-dimensional (both longitudinal and lateral) vehicle interaction by design;
- PR is grounded in the actual behaviour of drivers in different situations;
- PR is context-dependent for varying traffic conditions and road geometries.

With real-world trajectory data collected at an unsignalised urban intersection, we generate interaction maps using TTC, PET, and PR for comparison. These maps provide an empirical assessment of vehicle interaction at the intersection.

The following sections are organised to first introduce different indicators (Sec. II), then show experiment results

[1] Yiru Jiao, Simeon C. Calvert, and Hans van Lint are with Department of Transport & Planning, Delft University of Technology, 2628 CN Delft, the Netherlands y.jiao-1@tudelft.nl

[2] Sander van Cranenburgh is with Transport and Logistics Group, Department of Engineering Systems and Services, Delft University of Technology, 2628 BX Delft, the Netherlands

on a real-world dataset (Sec. III) with discussion (Sec. IV), and finally recap this study briefly (Sec. V).

II. Methods

A. Proximity resistance

Proximity resistance (PR) is termed to describe the (dis)comfort experience drivers undergo when vehicle spacing changes. This concept originates from driver space, which is an extension of pedestrians' personal space [19,20]. Intrusion into driver space (i.e., another vehicle or object moving closer than a driver's desired distance) causes discomfort, prompting drivers to maintain varying distances from others. By inferring the desired distance (i.e., critical spacing), PR can characterise drivers' two-dimensional spacing behaviour. This subsection briefly presents the representation of PR and its inference from vehicle trajectories, as shown in Fig. 1. Our previous study [18] is referred to for more details.

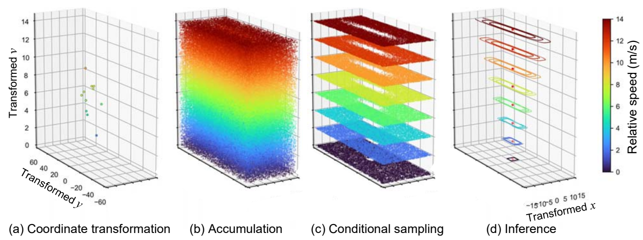

Fig. 1. Method structure of proximity resistance inference

For two vehicles i and j that are potentially interacting with each other, we firstly transform their coordinates into a system where i is at the origin and the y-axis points to the direction of their relative velocity. This coordinate transformation creates a normalised reference for vehicle pairs in different situations to be compared and aggregated. The aggregation of vehicles' relative states, as shown in Fig. 1(b) and (c), forms different empty spaces under varying relative speeds. We use proximity resistance as defined in eq. (1) to describe these empty spaces, which can quantify the varying levels of discomfort caused from driver space intrusion into a value between 0 and 1.

$$p(x,y|\boldsymbol{\theta}) = \exp\left(-\left|\frac{x}{r_x}\right|^{\beta_x} - \left|\frac{y}{r_y}\right|^{\beta_y}\right), \tag{1}$$

where each element of $\boldsymbol{\theta} = (r_x, r_y, \beta_x, \beta_y)^\top$ has two components:

$$\begin{cases} \theta = \dfrac{1+\mathrm{sgn}(x)}{2}\theta^+ + \dfrac{1-\mathrm{sgn}(x)}{2}\theta^- \text{ for } \theta = r_x, \beta_x, \\ \theta = \dfrac{1+\mathrm{sgn}(y)}{2}\theta^+ + \dfrac{1-\mathrm{sgn}(y)}{2}\theta^- \text{ for } \theta = r_y, \beta_y. \end{cases} \tag{2}$$

Higher values of $p(x,y)$ indicate increased discomfort. The representation of proximity resistance encodes two aspects of spacing change. Firstly, the parameters $\boldsymbol{r} = \{r_x^+, r_x^-, r_y^+, r_y^-\}$ determine the critical spacing in different directions, where $p = e^{-1}$ and $\boldsymbol{r}$ defines driver space boundary where proximity resistance changes most rapidly. Secondly, the parameters $\boldsymbol{\beta} = \{\beta_x^+, \beta_x^-, \beta_y^+, \beta_y^-\}$ determine how fast the transition between comfort and discomfort goes across the boundaries in different directions. Vehicle spacing is influenced by the movement states of interacting vehicles, the traffic situation they are in, as well as the driving preference of their drivers. Consequently, $\boldsymbol{\theta}$ differ given samples of vehicles in various scenarios.

The inference of $\boldsymbol{\theta}$ is achieved by estimating the density of aggregated vehicle pair presence. In each pair of vehicles, one is considered as an ego vehicle and the other as a vehicle in the surrounding. We aggregate all vehicle pairs in the same scenario where they have similar relative speeds. In this way, the ego vehicles together serve as an average ego vehicle, and the vehicles in the surrounding collectively shape a driver space in the scenario. With $\boldsymbol{\theta}$ inferred in different scenarios, we can calculate PR for vehicle pairs to determine the extent to which their spacing is too close.

B. Two dimensional Time-to-Collision

Ward et al. [21] highlighted the infinite possible paths for drivers at intersections, which necessitates considering TTC in a two-dimensional plane. They then introduce a method based on the change of the shortest distance between two approaching vehicles. Building on similar thoughts, Venthuruthiyil et al. [14] further refined Ward et al.'s method. They incorporated finer-grained movement variables such as acceleration and steering rate, and explicitly stated the implicit assumption in [21] that velocity needs to take the component along the shortest distance direction.

The method proposed in [14] is computationally demanding to apply to a large amount of data. Firstly, it requires vehicles' accelerations. Obtaining smooth and accurate acceleration data necessitates high-quality trajectories, since measurement errors propagate and increase with differentiation. Secondly, the calculation of the shortest distance in this method is challenging to vectorise, which results in increased processing time as the data volume grows.

In this study, we regard 2D-TTC as the time remaining until the bounding boxes of two vehicles touch each other. Firstly, we compute the distance to collision (DTC) as the minimum distance between the bounding boxes of vehicles along the direction of their relative velocity. Then we compute 2D-TTC as

$$TTC = \begin{cases} \dfrac{DTC}{\|\boldsymbol{v}_i - \boldsymbol{v}_j\|}, & DTC \neq \inf \\ \inf, & DTC = \inf \end{cases} \tag{3}$$

Compared to existing methods, our approach[1] streamlines the determination of whether two vehicles are approaching each other, and facilitates rapid computation for large amounts of data as it easily allows for vectorised computation. This increases its suitability for assessing vehicle interaction in practice.

[1]We have open-sourced the algorithm on: https://github.com/Yiru-Jiao/Two-Dimensional-Time-To-Collision

C. Post-Encroachment-Time

By definition, PET measures the time difference between when the tail of one vehicle clears a conflict zone and when the head of another vehicle enters the same conflict zone. In this study, we consider conflict zone as the intersection area of two crossing trajectories. Trajectory crossing may also occur if a vehicle is following another and their trajectories overlap. To filter crossing trajectories that are not overlapping, the trajectory of one vehicle i needs to intersect with the trajectory of another vehicle j, as well as two 3-meter (approximate lane width) buffers to the left and right. As shown in Fig. 2, this means that the trajectories of vehicle i and vehicle j need to have three intersections of $\{A, C, B\}$ or $\{D, C, E\}$ to be considered as crossing trajectories.

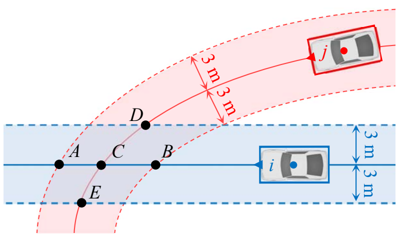

Fig. 2. Illustration of detecting conflict zone for computing PET

D. Vehicle interaction identification

These three indicators (i.e., PR, TTC, and PET) measure different quantities for a vehicle i and another vehicle j during time moment t_i and t_j (for PR and TTC, $t_j = t_i = t$) to signify vehicle interaction. There is not necessarily a value that draws the line between interaction and non-interaction. Instead, a threshold when the probability of interacting is greater than the probability of not interacting makes more sense. As such, whether i and j are interacting with each other is distinguished by comparing the indicator values (i.e., PR, TTC, and PET) with their corresponding thresholds denoted as PR*, TTC*, and PET*.

These indicators identify vehicle interaction from different perspectives, which are explained in Table I.

TABLE I

PERSPECTIVE COMPARISON BETWEEN PR, TTC, AND PET

Indicator	**Perspective:** vehicle i and j are interacting if
PR	the spacing between i and j is smaller than typically desired, i.e., PR$(i, j, t) >$ PR*
TTC	i and j are going to collide if their movements do not change, i.e., TTC$(i, j, t) <$ TTC*
PET	i and j pass their conflict zone within a short time gap, i.e., PET$(i, j, t_i, t_j) <$ PET*

While all three indicators are designed to account for the lateral component of vehicle dynamics, they do not directly differentiate between interacting longitudinally or laterally. To better observe their differences in identifying vehicle interaction in empirical analysis, we use the following condition to separate longitudinal and lateral interactions. When the angle between the heading directions of i and j is smaller than 5 degrees or larger than 175 degrees, they are considered to interact only in the longitudinal direction (e.g., car following and head-on approaching); otherwise, their interaction is considered to involve the lateral direction as well (e.g., lane-changing and turning).

III. RESULTS

A. Dataset and threshold selection

We compute the interaction indicators (PR, TTC, PET) at an unsignalised intersection referred to as *GL*, which is part of the trajectory dataset INTERACTION [22]. This dataset was collected in 2019 in the USA using drones that recorded videos of vehicle movement. At the intersection *GL*, 10,510 vehicles were recorded in 4.34 hours at a frequency of 10Hz.

The indicator thresholds are chosen as follows. For PR, we select the resistance level at critical spacing (i.e., e^{-1}) as PR*, identifying 88,742 interaction moments of (i, j, t) where PR(i, j, t)>PR*. According to [15,17,23], TTC* and PET* are both typically selected ranging from 1 s to 5 s, and values less than 1 s mean very critical situations. As interaction is considered as more general situations that involve conflicts, we determine TTC* and PET* to be both 4 s. Then we extract 90,273 interaction moments of (i, j, t) where TTC(i, j, t)<TTC*; and 59,568 interaction moments of $(i, j, t$ between t_i and $t_j)$ where PET(i, j, t_i, t_j)<PET*.

B. Interaction map

Based on the locations of the interaction moments, we generate interaction maps at the intersection *GL*. Specifically, we divide the intersection into 2×2 m^2 grids, then count the number of interaction moments in each grid, and calculate interaction rate as the proportion of interaction moments among all moments passing though the grid. Fig. 3 displays the generated interaction maps. Each column of subplots shows the maps based on different indicators, and each row of subplots shows the maps of different interaction types.

The figure shows clear differences between the maps and have various hotspots of higher interaction frequency. In the following subsections, we will explain the differences in more details.

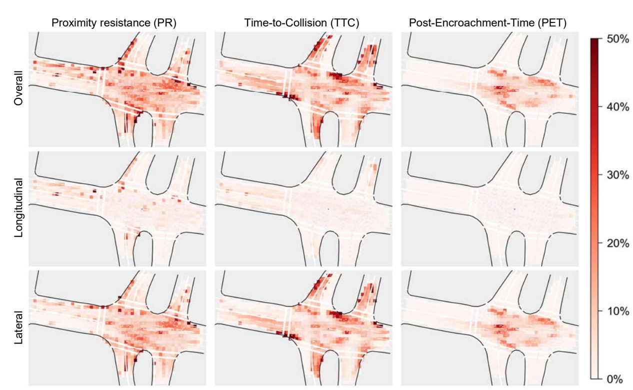

Fig. 3. Interaction maps generated using different indicators

C. Interaction rates in different sections

To further examine the distribution of vehicle interaction across the intersection and compare the results quantitatively, we divide *GL* into 9 sections according to its geometry and traffic directions. They are, as depicted in Fig. 4, (a) main road entry lane, (b) main road exit lane, (c) left-upper entry lane, (d) left-upper exit lane, (e) left-lower exit lane, (f) left-lower entry lane, (g) right entry leg, (h) right exit leg, and (i) inside *GL*.

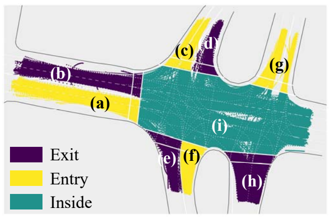

Fig. 4. Section division of the intersection *GL*

In Table II, we compare the interaction rates (IR) for different sections (abbreviated as Sec.) identified using PR, TTC, and PET. Here, IR is the ratio of interaction moments to the total number of moments in each section, rather than an average of the interaction rates across the grids within the section. Further, the proportion of longitudinal (abbreviated as Lon) and lateral (abbreviated as Lat) interaction among the identified interaction moments are also presented.

TABLE II
INTERACTION RATE STATISTICS AT DIFFERENT SECTIONS

Sec.	PR IR (%)	PR Lon (%)	PR Lat (%)	TTC IR (%)	TTC Lon (%)	TTC Lat (%)	PET IR (%)	PET Lon (%)	PET Lat (%)
(a)	<u>2.45</u>	70.41	29.59	11.53	17.02	82.98	1.61	1.29	98.71
(b)	8.79	59.80	40.20	5.83	62.25	37.75	0.09	57.69	42.31
(c)	6.65	28.88	71.12	11.12	5.80	94.20	0.38	4.23	95.77
(d)	3.60	2.43	97.57	<u>0.04</u>	100.00	0.00	<u>0.00</u>	NaN	NaN
(e)	7.01	1.44	98.56	0.66	33.66	66.34	0.20	0.00	100.00
(f)	**16.51**	33.31	66.69	**15.42**	7.26	92.74	1.40	0.48	99.52
(g)	8.65	18.22	81.78	11.83	7.18	92.82	0.63	0.00	100.00
(h)	6.72	3.28	96.72	5.50	2.99	97.01	<u>0.00</u>	0.00	100.00
(i)	12.53	17.55	82.45	10.36	10.90	89.10	**7.48**	4.70	95.30
All	10.17	25.47	74.53	10.37	12.80	87.20	3.47	58.49	41.51

The three indicators identify different sections with the highest and the lowest frequency of vehicle interaction. PR and TTC both identify (f) left-lower entry lane as having the most frequent interaction, while PET points to (i) inside *GL*. For the sections with infrequent vehicle interaction, PR identifies (a) main road entry lane, TTC highlights (d) left-upper exit lane, and PET indicates to (d) left-upper exit lane and (h) right exit leg.

Collectively considering Fig. 3 and Table II, confirmations and contradictions can be observed for vehicle interaction between the three methods. The confirmations include:

- longitudinal interaction predominantly occurs than lateral interaction in (b) main road exit lane and (c) left-upper entry lane;
- there are more lateral interaction than longitudinal interaction in (e) left-lower exit lane, (f) left-lower entry lane, (g) right entry leg, (h) right exit leg, and (i) inside the intersection.

The contradictions, on the other hand, include:

- PR indicates more longitudinal interaction in (a) main road entry lane, while TTC and PET suggest the opposite;
- PR reveals more lateral than longitudinal interaction in (d) left-upper exit lane, while TTC indicates longitudinal ones only.

D. Identification bias of PET and TTC

The contradictions stated above are justified as these indicators identify vehicle interaction from different perspectives (as explained in Table I). This subsection analyses in more depth on the methodological limitations of PET and TTC.

Looking back at Table II, PET identifies significantly less interactions in entry and exit lanes or legs. This is because we define conflict zone by crossing trajectories, which predominantly happen inside an intersection. One can also define conflict zone as any area at the intersection, and then PET can be understood as an extended concept of time headway. However, that would overestimate interaction because people can maintain short time headway during car-following, and in contrast, need more time to coordinate a conflict.

Regarding TTC, we need to look again at the interaction maps in Fig. 3. As marked in Fig. 5, TTC is sensitive to identify vehicle interactions at curved margins and when the vehicles are turning, in comparison to PR and PET. Turning and merging into exiting traffic may incur more frequent interactions, however, TTC cannot identify them completely. Situations at such as (b) main road exit lane and (h) right exit leg are ignored. We therefore suggest that this is because TTC solely considers the current velocities of vehicles and does not account for upcoming turn. In these turning scenarios, however, interactions (potential conflicts) are not necessarily in the direction of their current velocities.

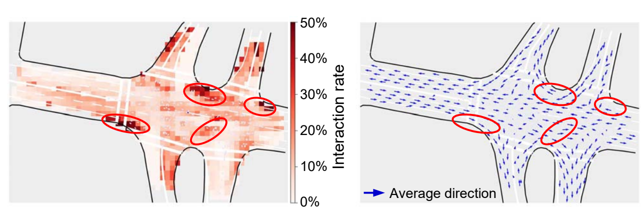

Fig. 5. High-frequency interaction areas identified by TTC

IV. Discussion

This section further investigates the difference of vehicle interaction identified by PR against by TTC and PET. In addition, the relation between PR and TTC is examined.

A. Speed distribution of interaction moments

In general, vehicle interactions happen at lower speeds. On the one hand, drivers adjust their behaviours according to other drivers' movement during interaction, resulting in speeds lower than the desired speeds in which they are free of interruption. On the other hand, lower speeds allow for adequate reaction time for drivers.

Fig. 6 shows the speed distribution of identified interaction moments. Compared with the speed distribution of all recorded moments in the dataset, all of PR, TTC, and PET show indicate less interaction at speeds higher than 7 m/s. At lower speeds, the interaction moments identified by TTC have a higher share in speeds between 1 m/s to 7 m/s; while PET identifies more interactions in speeds between 2 m/s and 6 m/s. These relatively higher shares of certain speeds could be due to the identification bias of TTC and PET, which is analysed in subsection III-D. Looking back at Fig. 3 and comparing them with Fig. 7, the hotspots of higher interaction frequency correspond to where the average speeds of passing vehicles are around 5 m/s.

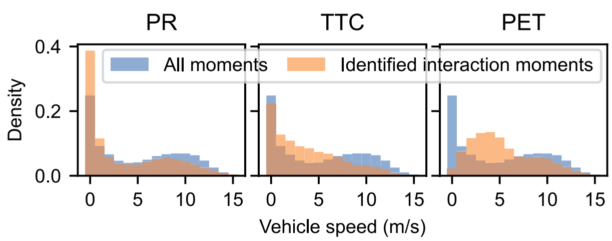

Fig. 6. Speed distribution of identified interacting moments

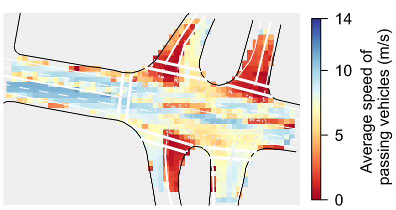

Fig. 7. Geographical speed distribution of all moments at the intersection

In contrast, interaction moments identified by PR have a relatively balanced speed distribution, but are more frequent in speeds smaller than 1 m/s. This is due to that PR identifies vehicle interaction from the perspective of spacing, and vehicles are more likely to maintain shorter spacing than preferred when they are in congestion or waiting other vehicles to pass first. For example, for the coordination of conflict at intersections, at least one of the two interacting drivers lower their speeds or stand still to yield the right-of-way to the other driver or each other. In the case where the right-of-way is clear and recognised by both of the interacting drivers, one may voluntarily wait while the other passes at a higher speed.

B. Interaction beyond conflicts

In Table I we argue that PR identifies vehicle interaction from a perspective different from potential conflicts and collisions. In Fig. 8, we use several real cases to instantiate the argument. The lines are vehicle trajectories, and the triangles at the end of trajectories point to moving directions. For time moments where PR$> e^{-1}$ but TTC< 4 s, we plot the rectangles to represent the vehicles. The more transparent the rectangle, the earlier the time moment is. We also denote the average TTC and average PR during these time moments.

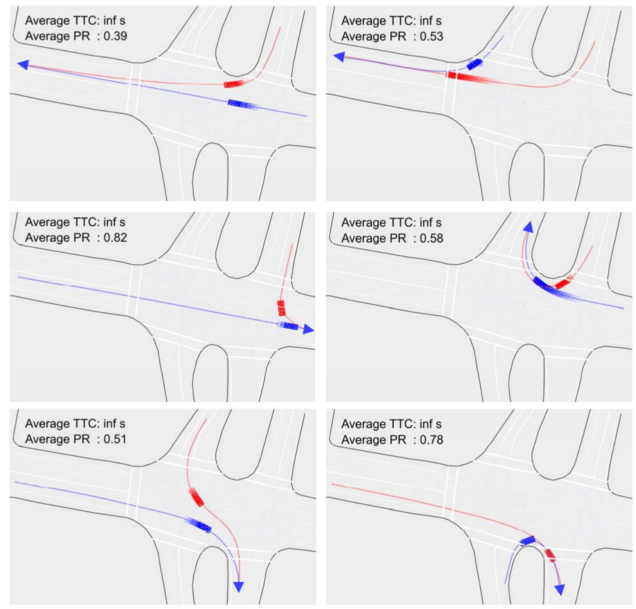

Fig. 8. Examples of interaction identified by PR but not by TTC or PET

These cases show how drivers coordinate with each other even though there is no imminent conflict. Such interactions cannot be identified by PET because there is not a single conflict point. Neither does TTC recognise these cases, as shown the infinite TTC values computed. PR indicates these interactions, however, it has its own limitations. The conceptual core of PR is to determine how often the current spacing is maintained for the current movement state (of all vehicles involved in the interaction), and this require a large amount of real-world data to learn. In this study, our method for computing PR maps relative movement states to a new coordinate system and aggregates similar states based on relative speeds only, thus simplifying the complexity of learning the patterns of spacing. This simplification, however, inevitably leads to false positives to a certain extent.

C. Relation between PR and TTC

As explained in subsection II-A, the computation of PR transforms the coordinates of vehicle pairs into a new system where the y-axis points to the direction of the relative velocity between the vehicles. When conditioned by the relative speed between two vehicles in a pair, the critical spacing inferred from accumulated vehicle presence serves as a threshold that distinguishes vehicle interaction. Vehicles in different relative speeds have different critical spacing as thresholds. These dynamic thresholds could be the reason for that PR avoids bias at curved margins and during turning at the intersection.

We therefore use $\hat{r}_y^+/|\boldsymbol{v}_{ij}|$, where $\hat{r}_y^+$ is the critical spacing along the relative velocity direction inferred during computing PR, as dynamic thresholds for TTC to identify vehicle interaction. Fig. 9 compares the interaction maps generated using TTC with a fixed threshold and dynamic thresholds.

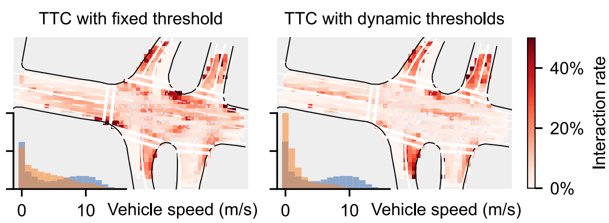

Fig. 9. Comparison between fixed and dynamic thresholds for identifying vehicle interaction using TTC

When using dynamic thresholds, the areas at curved margins and the turning near the right exit leg are no longer identified as hotspots with overly-high frequency of vehicle interaction. This suggests that dynamic thresholds can contribute to avoid identification bias of TTC during vehicle turning. Fig. 9 also shows the speed distrtibution of interaction moments. Compared to the identification with a fixed threshold, a larger share of vehicle interactions are at speeds lower than 3 m/s when using dynamic thresholds.

V. Conclusion

In this paper, we propose the use of proximity resistance (PR) for two-dimensional vehicle interaction identification from the perspective of critical spacing, and thoroughly compare vehicle interactions identified by PR and conflict indicators such as Time-to-Collision (TTC) and Post-Encroachment-Time (PET). The empirical analysis carried out at an unsignalised urban intersection demonstrates that PR can avoid certain identification bias and indicate cooperative interaction between vehicles. We highlight that vehicle interaction is not only a prelude before traffic conflicts, but also crucial for resolving conflicts and preventing critical cases of driving safety. By comparing vehicle interactions identified using PR, TTC, and PET, this study advances towards more comprehensive understanding of vehicle interaction at urban intersections.

Acknowledgment

This work is supported by the TU Delft AI Labs programme.

References

[1] J. Zhao, V. L. Knoop, and M. Wang, "Microscopic traffic modeling inside intersections: Interactions between drivers," *Transportation Science*, vol. 57, no. 1, pp. 135–155, 2022.

[2] V. Shepelev, A. Glushkov, A. Gritsenko, D. Nevolin, and A. Vorobyev, "Assessing the traffic capacity of urban road intersections," *Frontiers in Built Environment*, vol. 8, 2022.

[3] J. Apeltauer, A. Babinec, D. Herman, and T. Apeltauer, "Automatic vehicle trajectory extraction for traffic analysis from aerial video data," *The International Archives of the Photogrammetry, Remote Sensing and Spatial Information Sciences*, vol. XL-3/W2, pp. 9–15, 2015.

[4] M. A. Khan, W. Ectors, T. Bellemans, D. Janssens, and G. Wets, "Unmanned aerial vehicle–based traffic analysis: Methodological framework for automated multivehicle trajectory extraction," *Transportation Research Record*, vol. 2626, no. 1, pp. 25–33, 2017.

[5] R. Krajewski, J. Bock, L. Kloeker, and L. Eckstein, "The highD dataset: A drone dataset of naturalistic vehicle trajectories on german highways for validation of highly automated driving systems," in *2018 21st International Conference on Intelligent Transportation Systems (ITSC)*, IEEE, 2018.

[6] X. Chen, Z. Li, Y. Yang, L. Qi, and R. Ke, "High-resolution vehicle trajectory extraction and denoising from aerial videos," *IEEE Transactions on Intelligent Transportation Systems*, vol. 22, no. 5, pp. 3190–3202, 2021.

[7] C. Hydén, "The development of a method for traffic safety evaluation: The swedish traffic conflicts technique," *Bulletin Lund Institute of Technology, Department*, no. 70, 1987.

[8] N. Saunier and T. Sayed, "Probabilistic framework for automated analysis of exposure to road collisions," *Transportation Research Record*, vol. 2083, no. 1, pp. 96–104, 2008.

[9] Å. Svensson and C. Hydén, "Estimating the severity of safety related behaviour," *Accident Analysis & Prevention*, vol. 38, no. 2, pp. 379–385, 2006.

[10] G. Markkula, R. Madigan, D. Nathanael, E. Portouli, Y. M. Lee, A. Dietrich, J. Billington, A. Schieben, and N. Merat, "Defining interactions: a conceptual framework for understanding interactive behaviour in human and automated road traffic," *Theoretical Issues in Ergonomics Science*, vol. 21, pp. 728–752, 2020.

[11] C. Oh and T. Kim, "Estimation of rear-end crash potential using vehicle trajectory data," *Accident Analysis & Prevention*, vol. 42, no. 6, pp. 1888–1893, 2010.

[12] Q. Meng and X. Qu, "Estimation of rear-end vehicle crash frequencies in urban road tunnels," *Accident Analysis & Prevention*, vol. 48, pp. 254–263, 2012.

[13] Y. Li, D. Wu, J. Lee, M. Yang, and Y. Shi, "Analysis of the transition condition of rear-end collisions using time-to-collision index and vehicle trajectory data," *Accident Analysis & Prevention*, vol. 144, p. 105676, 2020.

[14] S. P. Venthuruthiyil and M. Chunchu, "Anticipated collision time (ACT): A two-dimensional surrogate safety indicator for trajectory-based proactive safety assessment," *Transportation Research Part C: Emerging Technologies*, vol. 139, p. 103655, 2022.

[15] S. S. Babu and P. Vedagiri, "Proactive safety evaluation of a multilane unsignalized intersection using surrogate measures," *Transportation Letters*, vol. 10, no. 2, pp. 104–112, 2016.

[16] L. N. Peesapati, M. P. Hunter, and M. O. Rodgers, "Can post encroachment time substitute intersection characteristics in crash prediction models?," *Journal of Safety Research*, vol. 66, pp. 205–211, 2018.

[17] M. Paul and I. Ghosh, "Post encroachment time threshold identification for right-turn related crashes at unsignalized intersections on intercity highways under mixed traffic," *International Journal of Injury Control and Safety Promotion*, vol. 27, no. 2, pp. 121–135, 2019.

[18] Y. Jiao, S. C. Calvert, S. van Cranenburgh, and H. van Lint, "Inferring vehicle spacing in urban traffic from trajectory data," *Transportation Research Part C: Emerging Technologies (in press)*, Aug. 2023.

[19] P. Marsh and P. Collett, "The car as a weapon," *ETC: A Review of General Semantics*, vol. 44, no. 2, pp. 146–151, 1987.

[20] D. A. Hennessy, S. Howard, and E. Carr, *Driver Space Preference: Differences Across Age, Gender and Traffic Conditions*, pp. 233–250. New York: Nova Science Publishers, 01 2011.

[21] J. R. Ward, G. Agamennoni, S. Worrall, A. Bender, and E. Nebot, "Extending time to collision for probabilistic reasoning in general traffic scenarios," *Transportation Research Part C: Emerging Technologies*, vol. 51, pp. 66–82, 2015.

[22] W. Zhan, L. Sun, D. Wang, H. Shi, A. Clausse, M. Naumann, J. Kümmerle, H. Königshof, C. Stiller, A. de La Fortelle, and M. Tomizuka, "INTERACTION Dataset: An INTERnational, Adversarial and Cooperative moTION Dataset in Interactive Driving Scenarios with Semantic Maps," *arXiv*, 2019.

[23] R. Jiang, S. Zhu, P. Wang, Q. Chen, H. Zou, and S. Kuang, "In search of the consequence severity of traffic conflict," *Journal of Advanced Transportation*, vol. 2020, pp. 1–15, 2020.